C_6-Ceramide Enhances Phagocytic Activity of Kupffer Cells through the Production of Endogenous Ceramides

Jong Min Choi[1,2], So Jung Chu[1,2], Kyong Hoon Ahn[1], Seok Kyun Kim[1], Jung Eun Ji[1], Jong Hoon Won[1], Hyung Chul Kim[1], Moon Jung Back[1], and Dae Kyong Kim[1,*]

Ceramide has been suggested to be not only a tumor-suppressive lipid but also a regulator of phagocytosis. We examined whether exogenous cell-permeable C_6-ceramide enhances the phagocytic activity of Kupffer cells (KCs) and affects the level of cellular ceramides. Rat KCs were isolated by collagenase digestion and differential centrifugation, using Percoll system. Phagocytic activity was measured by FACS analysis after incubating KCs with fluorescence-conjugated latex beads, and the level of cellular ceramide was analyzed by liquid chromatography tandem-mass spectrometry (LC-MS/MS). In this study we found that permeable C_6-ceramide increases the cellular levels of endogenous ceramides via a sphingosine-recycling pathway leading to enhanced phagocytosis by KCs.

INTRODUCTION

Systemic macrophages are responsible for the phagocytosis of most foreign material in the circulation. Kupffer cells (KCs) have the greatest capacity for phagocytosis (Yano et al., 2004). KCs represent an important component of innate immunity, which is the initial and rapid response to potentially dangerous stimuli (Bilzer et al., 2006).

Structural components of membranes, Sphingolipids, regulate cell-cell and cell-substrate interactions, proliferation, and differentiation. Further, members of this diverse group of lipids have emerged as a novel class of signaling molecules that also regulate phagocytosis. The mechanisms by which sphingolipids exert these effects remain incompletely defined (Blackwood et al., 1996; Hinkovska-Galcheva et al., 1998; Mitsutake et al., 2004).

Ceramide is generated either *via* a *de novo* pathway, in which serine-palmitoyltransferase (SPT) acts as a rate-limiting enzyme, or via the sphingomyelin (SM) pathway, in which sphingomyelinase (SMase) directly hydrolyzes SM (Hannun, 1996). Ceramide is known to be involved in cellular proliferation (Mitoma et al., 1998), differentiation (Okazaki et al., 1989; Riboni et al., 1995), growth arrest (Jayadev et al., 1995), and apoptosis (Kolesnick and Kronke, 1998). Newly identified functions of ceramide in domain coalescence, receptor clustering, and vesicle formation and fusion also conform to its important role as a membrane structural component (van Blitterswijk et al., 2003).

Ceramide has recently been suggested to be a modulator of phagocytosis (Li et al., 1999). Ceramide is generated during the phagocytosis of antibody-coated erythrocytes by polymorphonuclear leukocytes (Hinkovska-Galcheva et al., 2005; Suchard et al., 1997). In addition, ceramide can be generated in either the outer or inner leaflet of liposomes, evoking endocytosis or blebbing of their membranes, respectively (Holopainen et al., 2000; Zha et al., 1998). Exogenously added C_6-ceramide is suggested to induce endocytic vesicle formation, causing enlarged late endosomes and lysosomes in mouse embryonic fibroblast cell lines (Li et al., 1999).

Approximately 80-90% of SM on plasma membrane is localized on the outer leaflet (Vance and Steenbergen, 2005). SM acts as a reservoir of lipid signaling molecules because it can be converted back to a ceramide by both neutral and acidic SMase (Tafesse et al., 2006). It is reported that the activity of acidic SMase is enhanced when phagocytic receptors are activated (Abdel Shakor et al., 2004).

In the present study, we examined whether cell-permeable C_6-ceramide enhances the phagocytic activity of KCs isolated from rat liver and affects the levels of cellular ceramides.

MATERIALS AND METHODS

Materials

C_6-ceramide (D-erythro-N-hexanoylsphingosine), C_6-dihydroceramide (D-erythro-N-hexanoyldihydrosphingosine), and fumonisin B_1 were purchased from Biomol Research Laboratories Inc. (USA). Fluorescein isothiocyanate (FITC)-conjugated anti-rat IgG (whole molecule), LPS, and *Escherichia coli* serotype O128:B12 were purchased from Sigma Chemical Co. (USA). Fluoresbrite YG microspheres (3 μm) and FITC-conjugated latex beads were purchased from Polysciences, Inc. (USA). Mouse anti-rat CD163 (ED2) was purchased from AbD Serotec (UK). Antibiotic-antimycotic solution containing 10,000 units/ml

[1]Department of Environmental and Health Chemistry, College of Pharmacy, Chung-Ang University, Seoul 156-756, Korea, [2]These authors contributed equally to this work.
*Correspondence: proteinlab@hanmail.net

penicillin, 10 mg/ml streptomycin sulfate, and 25 μg/ml ampho-tericin B in 0.85% NaCl was purchased from Welgene (Korea). A 20-G catheter, 60-mm plastic culture dish, and 70-μm cell strainer were purchased from BD Biosciences (USA). Ca^{2+}/Mg^{2+}-free Hank's balanced salt solution (CMF-HBSS), fetal bovine serum (FBS), and RPMI 1640 media were purchased from Invitrogen (Korea). A zolazepam and tiletamine mixture (Zoletil) was purchased from Virbac Laboratories (France). Xylazine-HCl (Rompun) was purchased from Bayer Korea Ltd. (Korea), and collagenase type IV and DNase I were purchased from Roche (Switzerland). Percoll was purchased from GE Healthcare Korea (Korea), and anti-mouse F4/80-allophyco-cyanin (APC) was purchased from Caltag Laboratories (USA). Mouse IgG (whole molecule) was purchased from Jackson ImmunoResearch Laboratories, Inc. (USA), and Cell Counting Kit-8 (CCK-8) was purchased from Dojindo (Japan).

Experimental animals

Male Sprague-Dawley rats (age, 7-8 weeks old and body weight, 240-280 g) was purchased from Orient Bio Inc. (Korea). The rats were fed a standard pellet diet and water *ad libitum*. They were kept on a 12-h light/dark cycle in an animal facility.

Methods

Isolation of Kupffer cells from rat liver

Rat KCs were isolated by collagenase digestion and differential centrifugation, using Percoll, as described elsewhere and with slight modifications (Ashwood-Smith and Farrant, 1980; Salmon and Kohl, 1996). In detail, animals were anesthetized with an intra-muscular injection of Zoletil-Rompun mixture (4:1). After cutting the abdomen open, the portal vein was cannulated with a 20-G catheter. Next, the liver was perfused with 200 ml of CMF-HBSS, followed by 0.005% DNase and 0.05% colla-genase type IV in 250 ml HBSS at a rate of 12 ml/min at 37°C. Subsequently, the liver was chopped with scissors and sus-pended in 50 ml of the above-described collagenase solution supplemented with DNase. The liver suspension was incubated for complete digestion at 37°C. After incubation for 30 min, the cell soup was passed through a 70-μm cell strainer to remove undigested portions. The cell suspension was centrifuged at 70 × g for 5 min at 4°C to sediment hepatocytes. The supernatant was centrifuged at 700 × g for 7 min at 4°C. Next, the pellet was resuspended in serum-free RPMI 1640 medium, layered on a density cushion of 25%/50% discontinuous Percoll and then centrifuged at 1,800 × g for 20 min at 4°C without applying the centrifuge brake. The cells floating at the boundary of the 2 Percoll layers were collected and washed in HBSS by centrifug-ing at 700 × g for 7 min at 4°C. Finally, the cells were sus-pended in RPMI 1640 medium containing 20% FBS and 1% antibiotic-antimycotic solution and plated in 60-mm plastic cul-ture dishes (Falcon, Becton Dickinson, USA). After incubation for 1 h at 37°C with 5% CO_2, non-adherent cells were removed by gently washing 3 times with serum free-RPMI 1640. The cells adhering to the dish were KCs. The concentration of the cells was adjusted to 1×10^6 cells/4 ml/plate, and the cells were then cultured in RPMI 1640 medium containing 20% FBS and 1% antibiotic-antimycotic solution in a humidified atmosphere of 5% CO_2 at 37°C.

Immunofluorescent staining

The purity of KCs was determined by ED-2 staining, according to a previously reported protocol (Eugenin et al., 2007). Cells were fixed in chamber slides with acetone-methanol (1:1) for 5 min at -20°C, washed 3 times with phosphate-buffered saline

(PBS), and blocked with PBS containing 10% FBS for 30 min at room temperature before incubation with mouse anti-ED-2 monoclonal antibody (1:50 dilution, over-night at 4°C, Serotec, UK). Subsequently, the cells were washed with PBS, incubated with FITC-conjugated anti-rat IgG (1:100 dilution, 1 h, room temperature, Sigma, USA) and observed under a fluorescence microscope (Leica DM 2000). All photographs were taken with a digital camera (Leica DFC 300 FX).

Cell viability assay

Cell viability was determined using a CCK-8 (Dojindo, Japan), and 2-(2-methoxy-4-nitrophenyl)-3-(4-nitrophenyl)-5-(2.4-disul-fophenyl)-2H-tetrazolium, monosodium salt (WST-8) was re-duced with cellular dehydrogenase to give an orange product, formazan. To assess cell viability, the cells (2×10^5 cells/well) were plated on a 96-well plate and pre-incubated for 24 h. Then, they were treated with or without the indicated concentrations of C_6-ceramide and incubated for ~96 h. After incubation, WST-8 solution was added for a final concentration of 10% (v/v). The converted orange product, formazan, was colorimetrically mea-sured in a Genius Pro EIA plate reader (Tecan, Switzerland) at 450 nm.

Phagocytosis assay

KCs (1×10^6 cells/well) were cultured in RPMI 1640 medium supplemented with 1% antibiotic-antimycotic solution and 10% FBS in a humidified atmosphere of CO_2 at 37°C. After 24 h, the medium was refreshed, and the KCs were incubated with FITC-latex beads (10 beads/cell) in 4 ml culture medium for 2 h. Subsequently, the medium was removed, and the adherent cells were washed twice with ice-cold PBS to eliminate non-ingested FITC-conjugated latex beads. Finally, the cells were scraped with a cell scrapper into 1 ml ice-cold PBS. Phagocytic activity was measured using flow cytometry after staining for cell surface markers.

Cell surface staining for FACS analysis

After incubation with FITC-conjugated latex beads, KCs were scraped into 1 ml ice-cold PBS. The cells were then centrifuged at 1,000 × g for 5 min at 4°C. Next, the cell pellets were resus-pended in 1 ml staining medium. Then, 2.23 μl ChromPure mouse IgG (whole molecule) was added to the suspension and allowed to incubate for 30 min at 4°C. Samples were centri-fuged at 1,000 × g for 5 min at 4°C, and the cell pellets were resuspended in 96 μl staining medium. In order to stain the KCs, 4 μl rat anti-mouse F4/80 monoclonal antibody conjugated to APC was added and incubated for 30 min at 4°C. The reaction was terminated by adding 1 ml of staining medium, and sam-ples were centrifuged at 1,000 × g for 5 min at 4°C. Finally, the pellets were resuspended in 400 μl staining medium for FACS analysis.

FACS analysis

FACS analysis was performed using a FACSCalibur (BD Bio-sciences, CA). Data on at least 5,000 events in Region 2 (Fig. 4) and FL1-H (FITC) fluorescence intensity in Region 1 (Fig. 4) were collected for each sample. The mean fluorescence inten-sity (MFI) was analyzed using CellQuest Pro software (BD Biosciences, USA). The intensity of the fluorescent signal was used to determine the number of beads engulfed per cell, and the MFI represented the phagocytic activity of KCs.

LC-MS/MS

Measurement of ceramide subspecies was performed by LC/MS/MS as described previously (Yoo et al., 2006). The HPLC
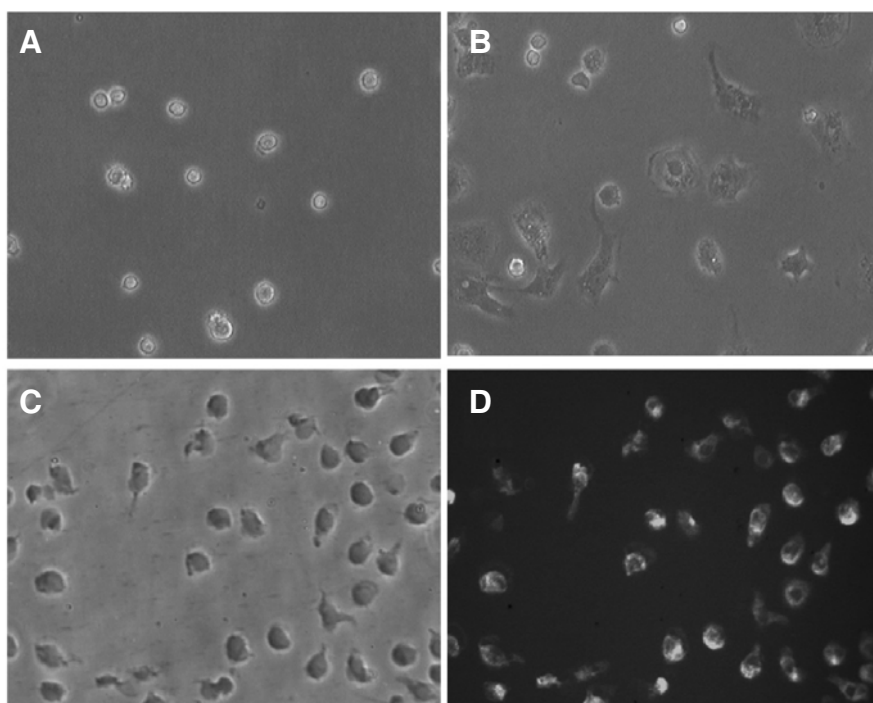
Fig. 1. Isolation and identification of Kupffer cells. (A) Freshly isolated KCs (ball-like shape). (B) KCs became larger and irregular after 24 h (200×). (C) Phase-contrast image taken after 1 day of culture. (D) Fluorescent image of cells stained with ED-2 (200×).

system consisted of an Agilent 1100 series binary pump and a column oven (Agilent technologies Inc., USA), combined with a CTC PAL autosampler (CTC Analytics, Switzerland). The analytical column was an X Terra MS C18 (2.0 × 50 mm, 3 μm; Waters Co.) and was kept at $45 \pm 0.5°C$ during the analysis. The mobile phase consisted of 0.1% formic acid and methanol buffered with 2 mM ammonium formate/tetrahy-drofuran (7/3, v/v; hereafter referred to as A) and 5 mM ammonium formate (pH 4.0)/methanol (9/1, v/v; hereafter referred to as B). For HPLC separation, a gradient program was used at a flow rate of 200 μl/min. The initial buffer composition was 80% mobile A and 20% mobile B, which was then linearly changed to 100% mobile A after 5 min and maintained for 4 min, and was then immediately reverted to the initial condition and maintained for 11 min. The run time of each experiment was 20 min. The HPLC system was coupled online to an SCIEX API 3000 triple-quadruple mass spectrometer (Applied Biosystems, Canada) equipped with a Turbo Ion Spray source. The mass spectrometer operated with unit resolution for both Q1 and Q3. Multiple reactions monitoring was employed using nitrogen as the collision gas with a dwell time of 150 ms for each transition. The optimal mass spectrometry values were obtained by manual tuning or automatic tuning, with each standard injected by a syringe pump. Data acquisition was confirmed using Analyst 1.4.1 software. The calibration curves for the sphingolipid standards were generated by plotting the peak area ratio (analyte/IS) versus the concentrations in the calibration standard samples by least-square linear regression.

RESULTS

Isolation of KCs
Rat KCs were isolated as described in Methods. The cell isolation method used in this study yielded approximately $7.5 \pm 0.2 \times 10^7$ KCs/liver in every experiment ($n = 10$). The freshly isolated cells had a ball-like shape and were 20-25 μm in diameter, when viewed under an optical microscope (CK40, Olympus, Japan) and with a digital camera (Moticam 2000) (Fig. 1A). Most cells adhered to the wall of the plastic culture dish after 1 h and became larger, more prominent, and showed typical macrophage morphology such as irregular shape after 24 h (Fig. 1B). The purity of the KCs fraction was consistently ≥ 90%, as determined on the basis of morphology and the results of ED-2 staining, which is a widely used method to detect KCs with the monoclonal antibody ED-2 (Figs. 1C and 1D).

Cell viability of the isolated KCs was measured using a CCK-8 at 24, 48, 72, and 96 h. The viability of the freshly isolated KCs (0 h) was considered to be 100% and used as the control. Data showed that 86% and 50% KCs were viable at 24 h and 96 h, respectively (Fig. 2). Cells cultured for 24 h (≥ 86% viability) were used in all experiments.

Effect of C_6-ceramide on the viability of KCs
To examine the cytotoxic effects of C_6-ceramide on KCs, the cells were treated with various concentrations of C_6-ceramide, ranging from 1 to 30 μM, for 2 h (Fig. 3). C_6-ceramide had no effect on cell viability up to 10 μM, whereas with 20 and 30 μM C_6-ceramide, cell viability decreased 10% and 49%, respectively. The concentrations that had no effects on viability were used in all experiments.

Effect of C_6-ceramide or C_6-dihydroceramide on phagocytosis by KCs
To investigate the effect of C_6-ceramide on the phagocytic activity of KCs, cells were treated with increasing concentrations of C_6-ceramide (1, 5, and 10 μM) or the same doses of C_6-dihydoceramide for 2 h in the presence of FITC-conjugated latex beads. To determine the phagocytic activity of KCs, the MFI was determined based on the proportion of F4/80-positive cells (KCs) that engulfed FITC-conjugated latex beads, and it was used to determine the number of beads engulfed per cell. LPS (1 μg/ml) was used as the positive control of phagocytosis.
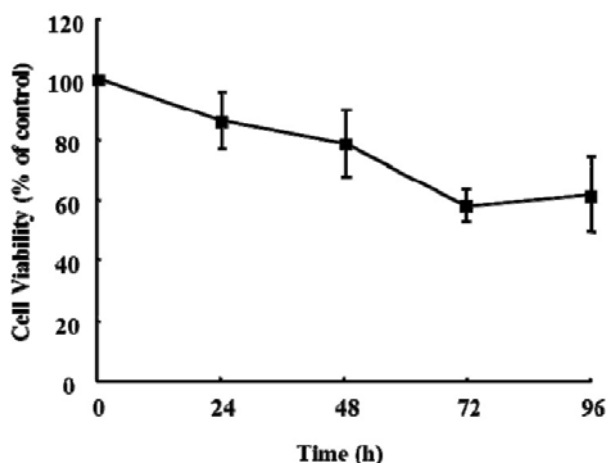
Fig. 2. Viability of Kupffer cells. KCs (2×10^5) were cultured in a 96-well plate, and the medium was changed daily. Cell viability was measured using a Cell Counting Kit-8 (CCK-8) at 0, 24, 48, 72, and 96 h after the cells were isolated from rat liver. The viability of KCs was more than 60% at 96 h. The viability of KCs at 0 h acted as the control. Data are expressed as mean $\pm$ SEM ($n = 3$).
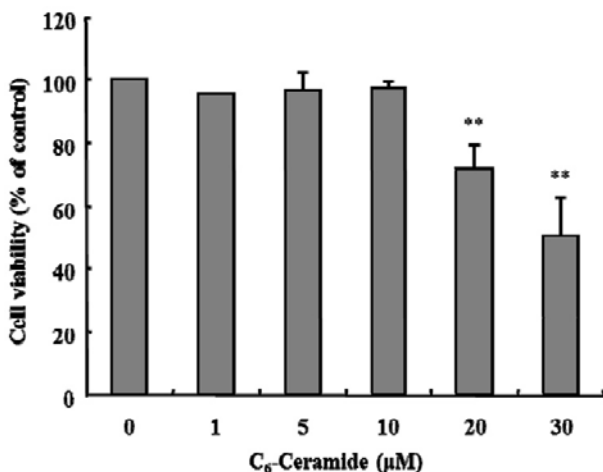

Fig. 3. Effect of C_6-Ceramide on the viability of KCs. KCs (2×10^5) were cultured in a 96-well plate. The cells were incubated with the indicated concentrations of C_6-ceramide for 120 min at 37°C. Viability was determined using a Cell Counting Kit-8 (CCK-8). The viability tests showed that $\geq$ 20 μM C_6-ceramide was toxic. Data are expressed as mean $\pm$ SEM ($n = 3$). Cells treated with each dose of C_6-ceramide were compared with the EtOH-treated control (**P < 0.005).

Phagocytic activity increased in the presence of C_6-ceramide (P < 0.05) (Fig. 5). Phagocytic activity increased to 40% and 50% of the control after treatment with 10 μM C_6-ceramide and LPS, respectively.

To evaluate the substrate specificity of phagocytosis, KCs were treated with C_6-dihydoceramide (1, 5, and 10 μM) in the presence of FITC-conjugated latex beads, but the phagocytic activity of KCs remained unaffected.
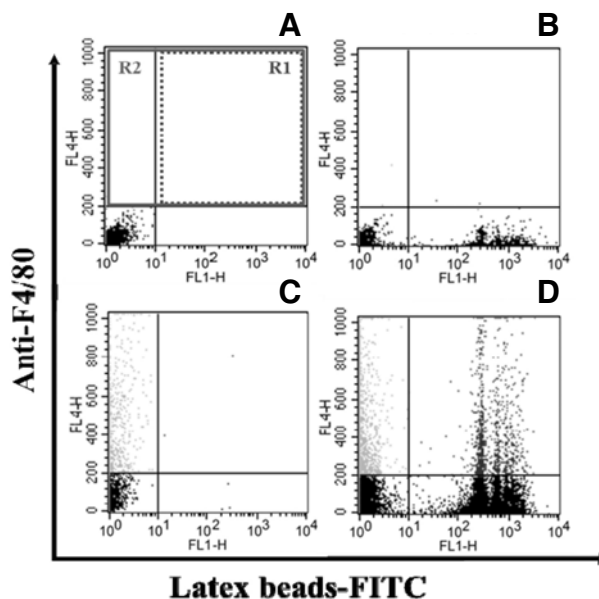

Fig. 4. FACS analysis of the phagocytic activity. Fluorescence intensity plots of FITC fluorescence (FL1-H channel, FITC-conjugated latex beads) vs. APC fluorescence (FL4-H channel, anti-F4/80-conjugated KCs) were analyzed. (A) Incubation without FITC-conjugated latex beads or anti-F4/80 monoclonal antibody. (B) Incubation with FITC-conjugated latex beads only. (C) Incubation with anti-F4/80 monoclonal antibody only. (D) Incubation with FITC-conjugated latex beads and anti F4/80 monoclonal antibody. R2 represents F4/80-positive KCs. R1 represents FITC-conjugated latex beads engulfed by KCs. Mean of fluorescence intensity (MFI) of R1 represents the phagocytic activity of KCs.
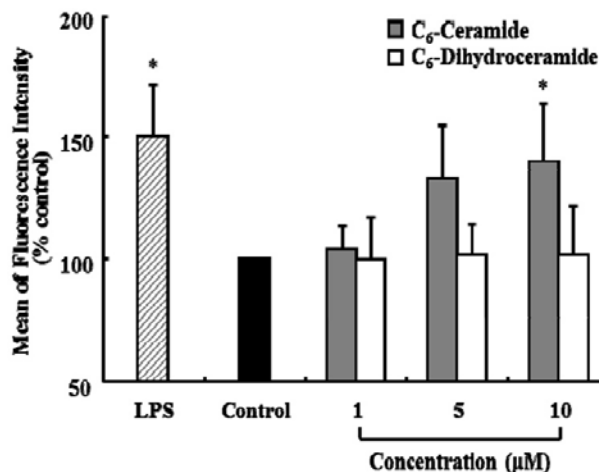

Fig. 5. Effect of exogenous C_6-ceramide or C_6-dihydroceramide on the phagocytic activity of Kupffer cells. KCs (1×10^6 cells/well) were incubated with FITC-conjugated latex beads (1×10^7 beads/well) in the presence of the indicated concentrations of C_6-ceramide or C_6-dihydroceramide for 120 min at 37°C. LPS (1 μg/ml) was used as the positive control for phagocytosis. Phagocytic activity was measured using flow cytometry. Data are expressed as mean $\pm$ SEM ($n = 3$). Cells treated with each dose of C_6-ceramide or C_6-dihydroceramide were compared with the control, which was treated only with EtOH (*P < 0.05).
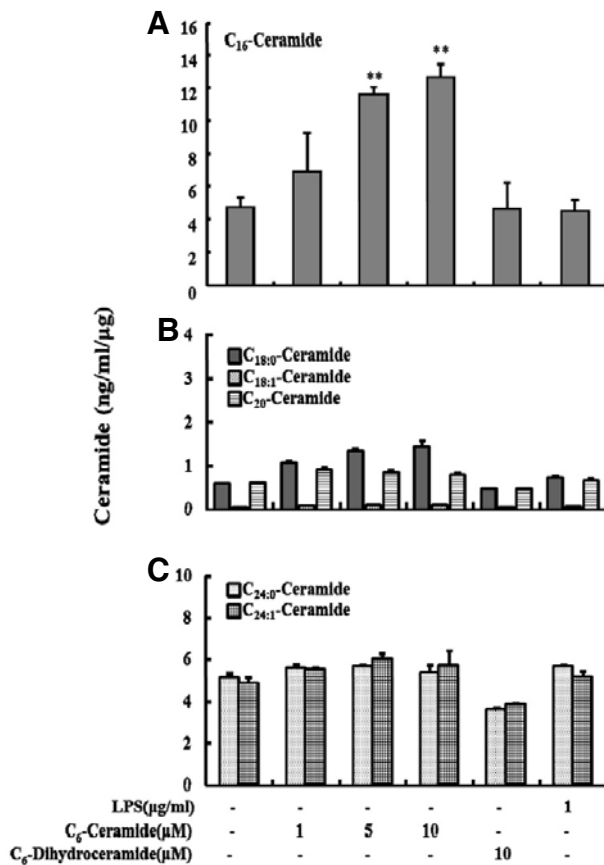
Fig. 6. Effect of exogenous C_6-ceramide or C6-Dihydroceramide on the production of endogenous ceramides in KCs. KCs (1×10^6 cells/well) were incubated with FITC-conjugated latex beads (1×10^7 beads/well) in the presence of C_6-ceramide (0, 1, 5, and 10 μM) or C_6-dihydroceramide (10 μM) or LPS (1 μg/ml) for 120 min at 37°C. The levels of endogenous ceramides were measured using liquid chromatography and tandem mass spectrometry (LC-MS/MS). Six endogenous ceramides were detected (A, C_{16}-cermide; B, $C_{18:0}$-ceramide, $C_{18:1}$-ceramide, and C_{20}-ceramide; C, $C_{24:0}$-ceramide and $C_{24:1}$-ceramide). Data are expressed as mean ± SEM (n = 3). Each figures share same label for X (LPS and ceramides treatment) and Y (ceramide concentration)-axis. Cells treated with each dose were compared with the control, which was treated only with EtOH (**P < 0.005).

Effect of C_6-eramide or C_6-dihydroceramide on the production of endogenous C_{16}-ceramide

To examine whether the enhanced response of phagocytosis to permeable C_6-ceramide was due to an alteration in the cellular levels of endogenous ceramides, KCs were treated with various concentrations of C_6-ceramide in the presence of FITC-conjugated latex beads for 2 h. Then, the levels of cellular C_{16}-ceramide, which is abundant in mammalian cells, were determined using LC-MS/MS. The results showed that treatment with C_6-ceramide increased endogenous C_{16}-ceramide levels in a dose-dependent manner and the level increased ~3-fold with 10 μM C_6-ceramide (P < 0.005) (Fig. 6A). Even though $C_{18:0}$-ceramide had the tendency to increase, the levels of $C_{18:0}$-ceramide, $C_{18:1}$-ceramide and C_{20}-ceramide were barely detectable; they were less than ~1 ng/ml/μg (Fig. 6B). The levels of $C_{24:0}$-ceramide and $C_{24:1}$-ceramide increased ~1.11-fold and
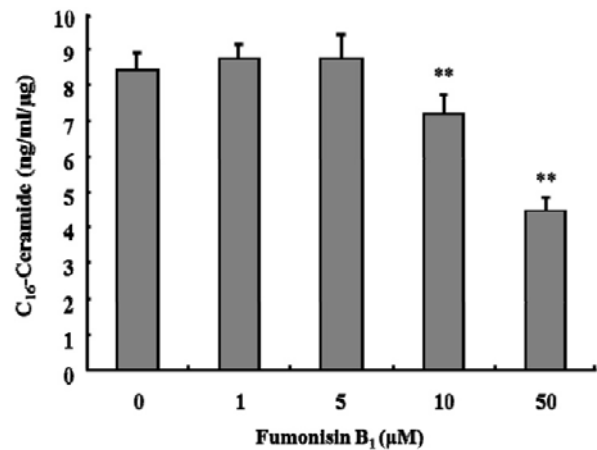

Fig. 7. Fumonisin B_1 inhibits the production of endogenous C_{16}-ceramide induced by exogenous C_6-ceramide. KCs (1×10^6 cells/well) were incubated with FITC-latex beads (10^7 beads /well) and 10 μM C_6-ceramide with several doses of fumonisin B_1 for 120 min at 37°C. Endogenous C_{16}-ceramide production was measured by liquid chromatography and tandem mass spectrometry (LC-MS). Data are expressed as mean ± SEM (n = 3). Cells treated with each dose of fumonisin B_1 were compared with the control, which was treated only with C_6-ceramide (**P < 0.005).

~1.27-fold respectively, but there were no significant change (Fig. 6C). And C_6-dihydroceramide, which has no effect on the phagocytic activity of KCs, caused no change in the level of endogenous C_{16}-ceramide.

Inhibition of C_6-ceramide-induced production and phagocytosis of C_{16}-ceramide by fumonisin B_1

To examine the biochemical pathway that mediates the production of endogenous long chain C_{16}-ceramide in response to C_6-ceramide, KCs were treated with fumonisin B_1, an inhibitor of ceramide synthase, in the presence of C_6-ceramide and FITC-conjugated latex beads. As shown in Fig. 7, the level of cellular C_{16}-ceramide significantly decreased by ~85% and ~54% in the presence of 10 μM and 50 μM fumonisin B_1, respectively, as compared with the control. Consistent with this result, 50 μM fumonisin B_1 almost completely inhibited the phagocytosis evoked with 10 μM C_6-ceramide in the presence of FITC-latex beads (Fig. 8).

These results suggest that the production of C_{16}-ceramide by C_6-ceramide may be due to the biochemical recycling of the sphingosine backbone of C_6-ceramide through deacylation/reacylation, which is a salvage pathway involving ceramide synthase.

DISCUSSION

Exogenous cell-permeable ceramide has been shown to induce cell differentiation, cell growth, and apoptosis (Bielawska et al., 1993; Dobrowsky and Hannun, 1992; Kim et al., 1991; Obeid et al., 1993; Okazaki et al., 1990). Moreover, recent studies have indicated that ceramide can mediate membrane fusion, especially antimicrobial responses such as phagocytosis and autophagy (Hinkovska-Galcheva et al., 2005; Park et al., 2008; Rohrbough et al., 2004).

KCs, the resident liver macrophages, represent approximately 80% of the total fixed macrophage population in the human body and have the greatest capacity for phagocytosis
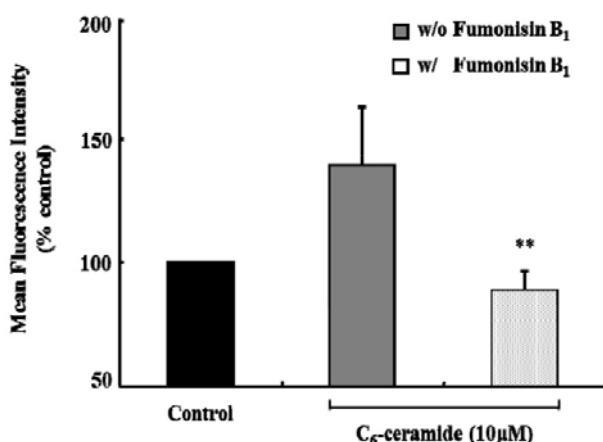
Fig. 8. Inhibitory effect of Fumonisin B_1 on exogenous C_6-ceramide-induced phagocytosis. KCs (1×10^6 cells/well) were incubated with FITC-conjugated latex beads (1×10^7 beads/well) at 10 μM C_6-ceramide with or without Fumonisin B_1 (50 μM) for 120 min at 37°C. Phagocytic activity was measured using flow cytometry. Data were expressed as mean ± SEM (n = 3). Inhibitory effect was demonstrated to compare with 10 μM C_6-ceramide treated group without Fumonisin B_1 (**P < 0.005).

among systemic macrophages (Cowper et al., 1990).

Asymmetric and heterogeneous properties of the biomembrane structure imply that lipid composition can play a significant role in the morphological changes of the membrane during phagocytosis. Several lines of evidence have shown that ceramide participates in the regulation of phagocytosis (Hannun, 1996; Tafesse et al., 2006). Exogenously added C_6-ceramide induces endocytic vesicle formation, causing the formation of enlarged late endosomes and lysosomes in mouse embryonic fibroblast cell lines (Li et al., 1999). Ceramide is also generated during the phagocytosis of antibody-coated erythrocytes by polymorphonuclear leukocytes (Hinkovska-Galcheva et al., 1998). However, whether ceramide participates in phagocytosis by disrupting membrane integrity remains almost unknown.

In the present study, we examined whether cell-permeable C_6-ceramide induces the phagocytic function of KCs isolated from rat liver and how C_6-ceramide induces phagocytosis. Flow cytometry and LC-MS/MS were used to investigate the phagocytic function of KCs and to measure changes in the cellular level of major endogenous ceramides.

Our data showed that C_6-ceramide increases phagocytic activity in a dose-dependent manner, as measured by the uptake of latex beads by KCs (Fig. 5). However, C_6-dihidyroceramide, which has no *trans*-double bond between C_4 and C_5 in its sphingosine base, had no effect on phagocytic activity. During C_6-ceramide-induced phagocytosis by KCs, changes in the cellular levels of endogenous ceramides were analyzed using LC-MS/MS. The levels of $C_{18:0}$-ceramide, $C_{18:1}$-ceramide, and C_{20}-ceramide were barely detectable; they were less than ~1 ng/ml/μg. The study focused on the levels of C_{16}-ceramide, $C_{24:0}$-ceramide, and $C_{24:1}$-ceramide. In particular, the level of C_{16}-ceramide increased ~3-fold, and this increase was significant. In contrast, the levels of $C_{24:0}$-ceramide and $C_{24:1}$-ceramide increased ~1.1-fold and ~1.3-fold, respectively (Fig. 6C). On the other hand, C_6-dihydroceramide caused no change in their cellular levels, further suggesting that changes in the levels of endogenous ceramides are responsible for the phagocytic activity of KCs. It should be noted that LPS, which is known to

be a positive inducer of phagocytosis (Nolan, 1981) in KCs, did not affect the level of C_{16}-ceramide (Fig. 6), suggesting that LPS-induced phagocytosis occurred via a different pathway, i.e., one that did not involve endogenous ceramides.

Fumonisin B_1, a mycotoxin produced by *Fusarium verticillioides*, is a specific and potent inhibitor of ceramide synthase. Fumonisin B_1 inhibits 50% of the activity of ceramide synthase (IC$_{50}$) at 0.1 μM for rat liver microsomes (Wang et al., 1991). In the present study, C_6-ceramide-induced production of C_{16}-ceramide (Fig. 7) and C_6-ceramide-induced phagocytosis (Fig. 8) was significantly inhibited by fumonisin B_1. These data strongly suggest that endogenous ceramides, in particular, C_{16}-ceramide, may be involved in phagocytosis.

Our data are in agreement with previous studies of the effects of permeable short-chain ceramides (Ogretmen et al., 2002; Sultan et al., 2006). Exogenously added short-chain ceramides undergo deacylation, followed by recycling of the sphingosine backbone by reacylation with a long-chain fatty acid. Such reacylation was inhibited by fumonisin B_1, suggesting that ceramide synthase may be involved in phagocytosis (Sultan et al., 2006). This study also suggests that a possible biochemical pathway, namely, the salvage pathway, may be involved.

In this study, we used dihydroceramide as a negative control for ceramide. Dihydroceramide was hydrolyzed to dihydrosphingosine (= sphinganine) by ceramidase as ceramide was hydrolyzed to shpingosine. Therefore, exogenous dihydroceramide can be hydrolyzed to increase the level of dihydrosphingosine. However, it is reported that ceramidase showed 10-fold higher rate of hydrolysis for ceramide than for dihydroceramide (El Bawab et al., 2002). And many studies have clearly shown that most of the biologic functions of ceramide are specific to ceramide and not dihydroceramide (Bielawska et al., 1993). Even though dihydrocermide was hydrolyzed to dihydrosphingosine, it must be saturated by dihydroceramide desaturase to be active ceramide. In our study, actually, dihydroceramide did not affect the phagocytosis and amount of endogenous ceramide in KCs.

Sugiura et al. (2002) reported that C_6-ceramide or C_{16}-ceramide but not C_6-dyhydroceramide can induce an increase in the activity of ceramide kinase, which is known to convert ceramide to C-1-P in a Ca-dependent manner. Further, C-1-P is formed in neutrophils after cell-permeable C_6-ceramide is added to the cells (Rile et al., 2003), and endogenous C-1-P can be generated during the phagocytosis of antibody-coated erythrocytes in human neutrophils (Hinkovska-Galcheva et al., 1998).

The precise mechanism by which ceramides that are endogenously produced by the salvage pathway affect KC-mediated phagocytosis remains unclear. Several possibilities can be proposed: One is that a long-chain ceramide produced by the salvage pathway or its metabolite, C-1-P, physically induces phagocytosis by disrupting membrane integrity by behaving like a fusogenic agent. Recent studies suggest that ceramide or C-1-P may play a role in fusion or making a pore on the biomembrane (Hinkovska-Galcheva et al., 1998; 2005). Another possibility is that endogenous cellular ceramides can stimulate a signal cascade by playing the role of second messengers. For example, ceramide is known to activate the GTPase of the Rho family and induce changes in the cytoskeleton (Yi et al., 2004). It is necessary to further investigate whether the generation of C_{16}-ceramide by exogenous C_6-ceramide regulates phagocytosis directly by affecting the physical state of the biomembrane or if another pathway is involved in this regulation and whether generated C_{16}-ceramide by C_6-ceramide induced phagocytosis after converted to Ceramide-1-phosphate.

In conclusion, our present study provides evidence that cell-permeable C_6-ceramide enhances phagocytosis of primary cultured KCs by participating in the generation of cellular ceramides via a sphingosine-recycling pathway.

REFERENCES

Abdel Shakor, A.B., Kwiatkowska, K., and Sobota, A. (2004). Cell surface ceramide generation precedes and controls FcgammaRII clustering and phosphorylation in rafts. J. Biol. Chem. *279*, 36778-36787.

Ashwood-Smith, M.J., and Farrant, J. (1980). Low temperature preservation in medicine and biology. (Pitman Medical, University Park Press).

Bielawska, A., Crane, H.M., Liotta, D., Obeid, L.M., and Hannun, Y.A. (1993). Selectivity of ceramide-mediated biology. Lack of activity of erythro-dihydroceramide. J. Biol. Chem. *268*, 26226-26232.

Bilzer, M., Roggel, F., and Gerbes, A.L. (2006). Role of Kupffer cells in host defense and liver disease. Liver Int. *26*, 1175-1186.

Blackwood, R.A., Transue, A.T., Harsh, D.M., Brower, R.C., Zacharek, S.J., Smolen, J.E., and Hessler, R.J. (1996). PLA2 promotes fusion between PMN-specific granules and complex liposomes. J. Leukoc. Biol. *59*, 663-670.

Cowper, K.B., Currin, R.T., Dawson, T.L., Lindert, K.A., Lemasters, J.J., and Thurman, R.G. (1990). A new method to monitor Kupffer-cell function continuously in the perfused rat liver. Dissociation of glycogenolysis from particle phagocytosis. Biochem. J. *266*, 141-147.

Dobrowsky, R.T., and Hannun, Y.A. (1992). Ceramide stimulates a cytosolic protein phosphatase. J. Biol. Chem. *267*, 5048-5051.

El Bawab, S., Usta, J., Roddy, P., Szulc, Z.M., Bielawska, A., and Hannun, Y.A. (2002). Substrate specificity of rat brain ceramidase. J. Lipid Res. *43*, 141-148.

Eugenin, E.A., Gonzalez, H.E., Sanchez, H.A., Branes, M.C., and Saez, J.C. (2007). Inflammatory conditions induce gap junctional communication between rat Kupffer cells both *in vivo* and *in vitro*. Cell Immunol. *247*, 103-110.

Hannun, Y.A. (1996). Functions of ceramide in coordinating cellular responses to stress. Science *274*, 1855-1859.

Hinkovska-Galcheva, V.T., Boxer, L.A., Mansfield, P.J., Harsh, D., Blackwood, A., and Shayman, J.A. (1998). The formation of ceramide-1-phosphate during neutrophil phagocytosis and its role in liposome fusion. J. Biol. Chem. *273*, 33203-33209.

Hinkovska-Galcheva, V., Boxer, L.A., Kindzelskii, A., Hiraoka, M., Abe, A., Goparju, S., Spiegel, S., Petty, H.R., and Shayman, J.A. (2005). Ceramide 1-phosphate, a mediator of phagocytosis. J. Biol. Chem. *280*, 26612-26621.

Holopainen, J.M., Angelova, M.I., and Kinnunen, P.K. (2000). Vectorial budding of vesicles by asymmetrical enzymatic formation of ceramide in giant liposomes. Biophys. J. *78*, 830-838.

Jayadev, S., Liu, B., Bielawska, A.E., Lee, J.Y., Nazaire, F., Pushkareva, M., Obeid, L.M., and Hannun, Y.A. (1995). Role for ceramide in cell cycle arrest. J. Biol. Chem. *270*, 2047-2052.

Kim, M.Y., Linardic, C., Obeid, L., and Hannun, Y. (1991). Identification of sphingomyelin turnover as an effector mechanism for the action of tumor necrosis factor alpha and gamma-interferon. Specific role in cell differentiation. J. Biol. Chem. *266*, 484-489.

Kolesnick, R.N., and Kronke, M. (1998). Regulation of ceramide production and apoptosis. Annu. Rev. Physiol. *60*, 643-665.

Li, R., Blanchette-Mackie, E.J., and Ladisch, S. (1999). Induction of endocytic vesicles by exogenous C(6)-ceramide. J. Biol. Chem. *274*, 21121-21127.

Mitoma, J., Ito, M., Furuya, S., and Hirabayashi, Y. (1998). Bipotential roles of ceramide in the growth of hippocampal neurons: promotion of cell survival and dendritic outgrowth in dose- and developmental stage-dependent manners. J. Neurosci. Res. *51*, 712-722.

Mitsutake, S., Kim, T.J., Inagaki, Y., Kato, M., Yamashita, T., and Igarashi, Y. (2004). Ceramide kinase is a mediator of calcium-dependent degranulation in mast cells. J. Biol. Chem. *279*, 17570-17577.

Nolan, J.P. (1981). Endotoxin, reticuloendothelial function, and liver injury. Hepatology *1*, 458-465.

Obeid, L.M., Linardic, C.M., Karolak, L.A., and Hannun, Y.A. (1993). Programmed cell death induced by ceramide. Science *259*, 1769-1771.

Ogretmen, B., Pettus, B.J., Rossi, M.J., Wood, R., Usta, J., Szulc, Z., Bielawska, A., Obeid, L.M., and Hannun, Y.A. (2002). Biochemical mechanisms of the generation of endogenous long chain ceramide in response to exogenous short chain ceramide in the A549 human lung adenocarcinoma cell line. Role for endogenous ceramide in mediating the action of exogenous ceramide. J. Biol. Chem. *277*, 12960-12969.

Okazaki, T., Bell, R.M., and Hannun, Y.A. (1989). Sphingomyelin turnover induced by vitamin D3 in HL-60 cells. Role in cell differentiation. J. Biol. Chem. *264*, 19076-19080.

Okazaki, T., Bielawska, A., Bell, R.M., and Hannun, Y.A. (1990). Role of ceramide as a lipid mediator of 1 alpha,25-dihydroxy-vitamin D3-induced HL-60 cell differentiation. J. Biol. Chem. *265*, 15823-15831.

Park, M.A., Zhang, G., Norris, J., Hylemon, P.B., Fisher, P.B., Grant, S., and Dent, P. (2008). Regulation of autophagy by ceramide-CD95-PERK signaling. Autophagy *4*, 929-931.

Riboni, L., Prinetti, A., Bassi, R., Caminiti, A., and Tettamanti, G. (1995). A mediator role of ceramide in the regulation of neuroblastoma Neuro2a cell differentiation. J. Biol. Chem. *270*, 26868- 26875.

Rile, G., Yatomi, Y., Takafuta, T., and Ozaki, Y. (2003). Ceramide 1-phosphate formation in neutrophils. Acta Haematol. *109*, 76-83.

Rohrbough, J., Rushton, E., Palanker, L., Woodruff, E., Matthies, H.J., Acharya, U., Acharya, J.K., and Broadie, K. (2004). Ceramidase regulates synaptic vesicle exocytosis and trafficking. J. Neurosci. *24*, 7789-7803.

Salmon, F., and Kohl, W. (1996). Use of fresh and cryopreserved hepatocytes to study the metabolism of pesticides in food-producing animals and rats. Xenobiotica *26*, 803-811.

Suchard, S.J., Hinkovska-Galcheva, V., Mansfield, P.J., Boxer, L.A., and Shayman, J.A. (1997). Ceramide inhibits IgG-dependent phagocytosis in human polymorphonuclear leukocytes. Blood *89*, 2139-2147.

Sugiura, M., Kono, K., Liu, H., Shimizugawa, T., Minekura, H., Spiegel, S., and Kohama, T. (2002). Ceramide kinase, a novel lipid kinase. Molecular cloning and functional characterization. J. Biol. Chem. *277*, 23294-23300.

Sultan, I., Senkal, C.E., Ponnusamy, S., Bielawski, J., Szulc, Z., Bielawska, A., Hannun, Y.A., and Ogretmen, B. (2006). Regulation of the sphingosine-recycling pathway for ceramide generation by oxidative stress, and its role in controlling c-Myc/Max function. Biochem. J. *393*, 513-521.

Tafesse, F.G., Ternes, P., and Holthuis, J.C. (2006). The multigenic sphingomyelin synthase family. J. Biol. Chem. *281*, 29421-29425.

van Blitterswijk, W.J., van der Luit, A.H., Veldman, R.J., Verheij, M., and Borst, J. (2003). Ceramide: second messenger or modulator of membrane structure and dynamics? Biochem. J. *369*, 199-211.

Vance, J.E., and Steenbergen, R. (2005). Metabolism and functions of phosphatidylserine. Prog. Lipid Res. *44*, 207-234.

Wang, E., Norred, W.P., Bacon, C.W., Riley, R.T., and Merrill, A.H., Jr. (1991). Inhibition of sphingolipid biosynthesis by fumonisins. Implications for diseases associated with Fusarium moniliforme. J. Biol. Chem. *266*, 14486-14490.

Yano, H., Kinoshita, S., and Kira, S. (2004). Effects of acute moderate exercise on the phagocytosis of Kupffer cells in rats. Acta Physiol. Scand *182*, 151-160.

Yi, F., Zhang, A.Y., Janscha, J.L., Li, P.L., and Zou, A.P. (2004). Homocysteine activates NADH/NADPH oxidase through ceramide-stimulated Rac GTPase activity in rat mesangial cells. Kidney Int. *66*, 1977-1987.

Yoo, H.H., Son, J., and Kim, D.H. (2006). Liquid chromatography-tandem mass spectrometric determination of ceramides and related lipid species in cellular extracts. J. Chromatogr. B Analyt. Technol. Biomed. Life Sci. *843*, 327-333.

Zha, X., Pierini, L.M., Leopold, P.L., Skiba, P.J., Tabas, I., and Maxfield, F.R. (1998) Sphingomyelinase treatment induces ATP-independent endocytosis. J. Cell Biol. *140*, 39-47.